Molecular Sensing with Hyperpolarized ^{129}Xe using Switchable Chemical Exchange Relaxation Transfer.

Francesco Zamberlan,[+][a] Clémentine Lesbats,[+][b] Nicola J. Rogers,[b] James L. Krupa,[a] Galina E. Pavlovskaya,[b] Neil R. Thomas,*[a] Henryk Faas,*[b] and Thomas Meersmann*[b]

Abstract: A new approach for hyperpolarized ^{129}Xe molecular sensors is explored using paramagnetic relaxation agents that can be deactivated upon chemical or enzymatic reaction with an analyte. Cryptophane encapsulated ^{129}Xe within the vicinity of the paramagnetic center experiences fast relaxation that, through chemical exchange of xenon atoms between cage and solvent pool, causes accelerated hyperpolarized ^{129}Xe signal decay in the dissolved phase. In this work, the relaxivity of **Gadolinium**^{III}-DOTA on ^{129}Xe in the solvent was increased eightfold through tethering of the paramagnetic molecule to a cryptophane cage. This potent relaxation agent can be 'turned off' specifically for ^{129}Xe through chemical reactions that spatially separate the **Gd**^{III} centre from the attached cryptophane cage. Unlike ^{129}Xe chemical shift based sensors, the new concept does not require high spectral resolution and may lead to a new generation of responsive contrast agents for molecular MRI.

Molecular imaging enables the *in vivo* detection of the spatial distribution of specific target molecules that serve as 'biomarkers' for organ physiology. Imaging of biomarkers allows for the early detection of disease, for better monitoring of treatment, and for drug development. Among the strategies to enable molecular MRI[1] the hyperpolarized (hp) ^{129}Xe biosensor concept pioneered by Pines, Wemmer, and co-workers[2] is a promising candidate due to xenon's non-toxicity, the simplicity of the corresponding NMR spectra, and its solubility in blood plasma and tissue.[3] Hp ^{129}Xe biosensors utilize an encapsulating agent, such as cryptophane cages, that can reversibly bind Xe atoms with fast rates of exchange. The large chemical shift range of ^{129}Xe leads to a distinguishable signal separation between encapsulated xenon atoms in the hydrophobic cavity and xenon in the solvent (not visible in Fig. 1b due to line broadening, see Fig. S2 in Supporting Information). Furthermore, cryptophanes can be functionalized with suitable bioactive ligands to serve as biosensor molecules that interact with a particular biomarker, typically a protein. The biosensor – biomarker interaction further alters the environment of the encapsulated ^{129}Xe, giving rise to a different chemical shift that can be observed by NMR spectroscopy. This was originally shown with biotin-functionalized cryptophane as a sensor for the protein avidin[2a] for which biotin has a very high affinity.

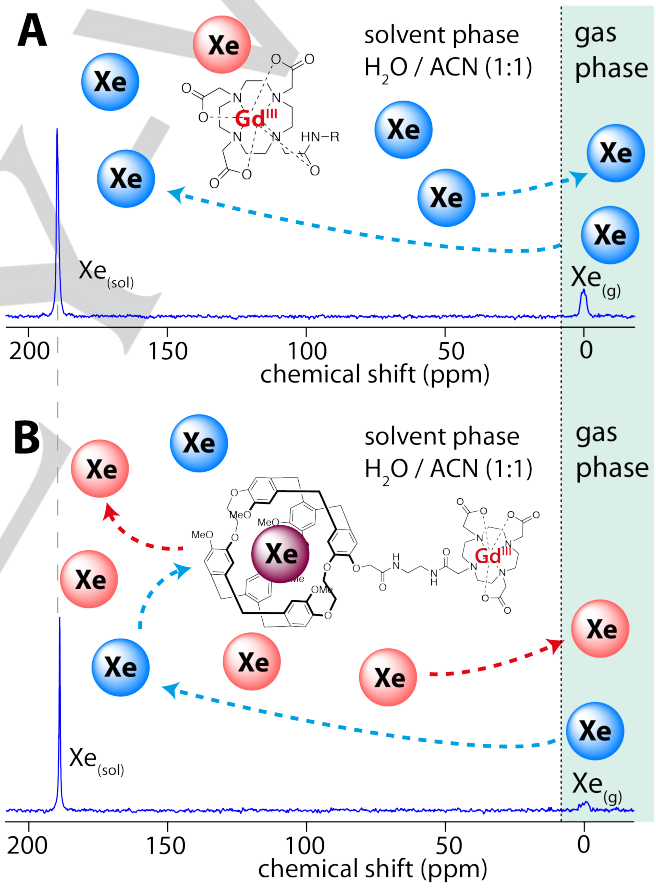

Figure 1. A) Hp ^{129}Xe NMR spectrum of a 1:1 v/v water/acetonitrile (H_2O/ACN) solution containing 0.33 mM **Gd**DOTA. The hp ^{129}Xe signal intensity of the dissolved phase (189.6 ppm) - and through exchange, the intensity of the gas phase (0 ppm) - is only moderately affected by the relaxation agent because the exposure time of the xenon atoms to the paramagnetic center is very limited. B) Hp ^{129}Xe NMR spectrum of 0.035 mM cryptophane-A tethered to **Gd**DOTA in H_2O/ACN solution. Encapsulated ^{129}Xe is not detected because of severe line broadening. This molecule serves as a strong relaxation agent, specifically for ^{129}Xe, due to prolonged duration of ^{129}Xe encapsulation in the close vicinity to the paramagnetic relaxation center. The effect of fast relaxation (or depolarization) of encapsulated hp ^{129}Xe is transferred via chemical exchange to the dissolved phase (189.3 ppm) where an accelerated decay of the ^{129}Xe$_{(sol)}$ signal is observed.

[a] Dr. F. Zamberlan[+], Mr. J. L. Krupa, Prof. N.R. Thomas
Centre for Biomolecular Sciences, School of Chemistry, University of Nottingham, Nottingham, United Kingdom
E-mail: Neil.Thomas@Nottingham.ac.uk

[b] Ms. C. Lesbats[+], Dr. N.J. Rogers[&], Dr. G.E. Pavlovskaya. Dr. H. Faas, Prof. T. Meersmann
Sir Peter Mansfield Imaging Centre, Division of Respiratory Medicine, School of Medicine, University of Nottingham, Nottingham, NG7 2RD, United Kingdom
E-mail: Henryk.Faas@Nottingham.ac.uk; Thomas.Meersmann@Nottingham.ac.uk

[&] Current address: Department of Chemistry, Durham University, South Road, Durham, DH1 3LE, United Kingdom

[+] These authors contributed equally.

Supporting information for this article is given via a link at the end of the document.

Hyperpolarized ^{129}Xe Chemical Exchange Saturation Transfer (HyperCEST)[2c] improves the hp ^{129}Xe biosensor detection limit by orders of magnitude.[4] HyperCEST is achieved by selective irradiation (i.e. saturation) at the NMR frequency of the encapsulated ^{129}Xe signal that depolarizes its hp spin state. Chemical exchange continuously transfers depolarized ^{129}Xe from the cage to the dissolved phase and accelerates the decay of the dissolved phase signal.

Molecular sensing with HyperCEST usually relies on the small ^{129}Xe chemical shift differences created by biosensor – biomarker interactions that are typically in the 2-3 ppm range, with exceptional cases up to 8 ppm.[6] Although hp ^{129}Xe biosensors enable a host of biomolecular NMR applications,[3a, 3b, 6-7] including *in vitro* MRI for cell tracking [8] and *in vivo* organ uptake of functionalized nanoparticles,[9] *in vivo* MRI usage in complex organisms such as vertebrates is generally limited by the achievable low spectral resolution. This is a limitation wherever chemical shift is required to distinguish between a binding (or cleaving) event and unspecific interaction (i.e. typically non-reacted sensors that are still present to a significant extent). A very promising advancement has been reported very recently that does not require high spectral resolution because the unspecific background was very small. HyperCEST enabled imaging of cell-surface glycans at nanomolar concentrations in live-cell bioreactors[5]. However, wherever the biosensor molecules interacting with biomarker molecules need to be distinguished from a significant amount of biosensors that have not been bound, cleaved, or otherwise reacted biomarker specifically, imaging will likely have to cope with small chemical shift differences between the two biosensor moieties.

This proof-of-concept study presents a different approach for hp ^{129}Xe biosensors, sketched in Fig. 1b, using paramagnetic relaxation instead of the chemical shift. Paramagnetic relaxation causes rapid decay of the hp signal. Paramagnetic metal centers are therefore usually avoided for hp MRI probes, except for the generation of negative contrast through shortened T_1, T_2, or T_2* times.[10] Note that upon submission of this manuscript, the authors learned that a paramagnetic relaxation based hp^{129}Xe biosensor concept has also been reported by Wemmer, Pines, and co-workers[11]. The new hp ^{129}Xe biosensor concept in this work utilizes 'switchable' paramagnetic relaxation. Chemical sensing will be based on chemical changes brought about by target molecules that 'deactivate' the responsive relaxation agent. Hp ^{129}Xe will be administered after sufficient time has passed to allow for any deactivation to occur that causes positive MRI contrasts. NMR relaxation studies with the model sensor CrA-**Gd**DOTA were used to gain insights into the magnitude of the relaxivity change and hence to explore the concept feasibility.

.

Results and Discussion. A 1:1 v/v mixture of water with acetonitrile (H_2O/ACN) was found to be an acceptable solvent for the model sensor, DOTA itself, and **Gd**^{III} but also for the xenon atoms. As shown in Fig. 2, the ^{129}Xe relaxation rates, $R_1 = 1/T_1$, were measured as function of the concentration of the various relaxation agents, [**Rx**], to determine the relaxivity of the respective agents. The relaxivity of **Gd**DOTA for ^{129}Xe$_{(sol)}$ was determined as R_1/[**Rx**] = 0.0515 $s^{-1}mM^{-1}$ (see Fig. 3). The approximately 150 fold reduced relaxivity of gadolinium for ^{129}Xe$_{(sol)}$ compared to that for H_2O protons (7.66 $s^{-1}mM^{-1}$ – see Fig. 3) is caused in part by xenon's lower gyromagnetic ratio γ that contributes to an approximately 13 fold reduced relaxivity due to the γ^2 dependence of paramagnetic relaxation.[12],[13] In addition, H_2O protons experience further accelerated relaxation because of direct coordination of water with the **Gd**^{III} center in DOTA complexes.[1]

A 1 mM **Gd**DOTA solution causes only slow hp ^{129}Xe$_{(sol)}$ relaxation, with T_1 = 19 s, that will have little effect on the overall ^{129}Xe relaxation behavior *in vivo*. For example, typical relaxation times for hp ^{129}Xe$_{(aq)}$ in blood range from approximately 2.7 to 7.9 s, depending on blood oxygenation.[14] In lung tissue and blood, rapid exchange with the gas phase prolongs the ^{129}Xe$_{(aq)}$ relaxation times up to 20 s.[13]

For CrA-**Gd**DOTA, where **Gd**DOTA is tethered to the cryptophane cage, the **Gd**^{III} relaxivity for ^{129}Xe$_{(sol)}$ increased more than 8 times to R_1/[**Rx**] = 0.416 $s^{-1}mM^{-1}$. The large relaxivity enhancement is likely caused by fast relaxation of encapsulated ^{129}Xe in close proximity to the paramagnetic **Gd**DOTA. Paramagnetic relaxation follows an r^{-6} dependence,[12] where r is the distance between the nuclear spin (here, of encapsulated ^{129}Xe) and the paramagnetic center. Chemical exchange between Xe in cages and solution transfers the relaxation effect and leads to accelerated R_1 rates for the dissolved phase ^{129}Xe$_{(sol)}$. The relatively small ^{129}Xe$_{(sol)}$ chemical shift dependence on [**Rx**] is listed in Fig. 3A and Fig. 3B for comparison.

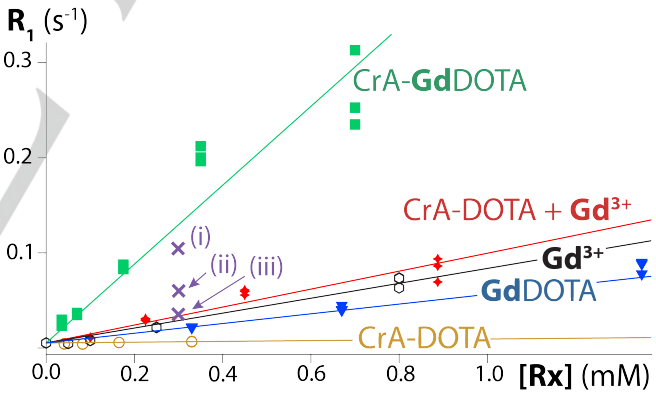

Figure 2. Relaxation rates, R_1, of dissolved phase ^{129}Xe$_{(sol)}$ in 1:1 v/v H_2O/ACN solution as a function of the concentration of various agents, [**Rx**], at 293 K and 9.4 T field strength. Note that CrA-DOTA + **Gd**$^{3+}$ (red data points and line) shows the relaxation data obtained more than 24 h after adding HCl to the solution with CrA-**Gd**DOTA, causing **Gd**$^{3+}$ to be expelled from the molecule. Data point (i) shows effect of CrA-**Gd**DOTA approximately 1 h after addition of HCl. (ii) After 24 h the reaction to CrA-DOTA + **Gd**$^{III}_{(sol)}$ was 86 % complete as determined by HPLC (see supporting material). (iii) Reaction is 96% complete after 96 h. Data points (i)-(iii) (i.e. crosses) are averages from three measurements – all other data are from single measurements. Relaxivity values are reported in Fig. 3.

The relaxivity of CrA-**Gd**DOTA for ^{1}H was very similar to that of **Gd**DOTA. This was expected from Solomon-Bloembergen-Morgan theory[12b] since the addition of the CrA group should have little effect on the number (q) of water molecules

coordinated to **Gd**^{III} or their residence time. Furthermore, the rotational correlation time associated with the relatively small CrA-**Gd**DOTA molecule is too short to significantly alter the relaxation behavior.

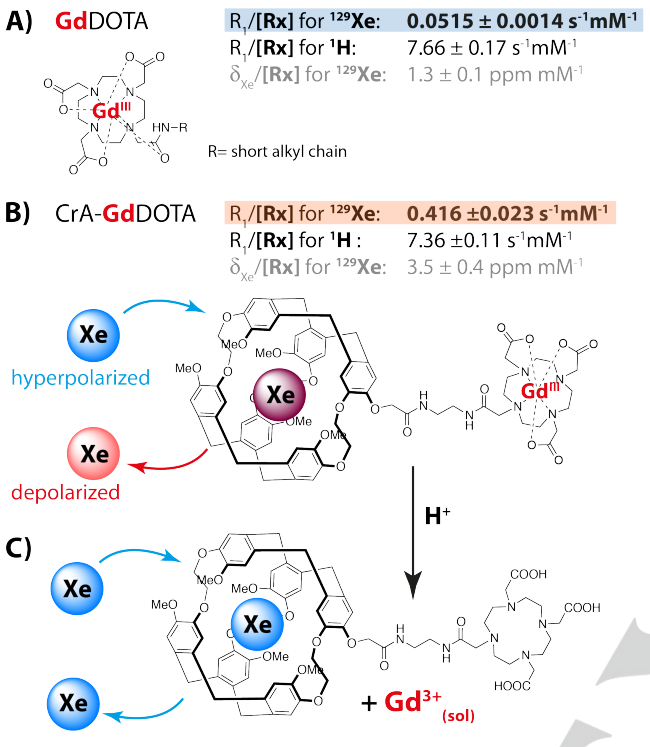

Figure 3. Relaxivity, R_1/[**Rx**], of various substances, **Rx**, for dissolved phase $^{129}Xe_{(sol)}$ and ^{1}H (of H_2O) at 293 K and 9.4 T in H_2O/ACN (1:1 v/v) solution. Relaxivity was determined from linear fitting of data in Fig. 2 with 0.0053 $s^{-1}mM^{-1}$ offset (i.e. experimental relaxivity of solvent). The dissolved phase $^{129}Xe_{(sol)}$ chemical shift δ_{Xe} dependence on [**Rx**] is obtained from linear fitting of $^{129}Xe_{(sol)}$ peak position using a 189.3 ppm (solvent) offset. A) Relaxivity of **Gd**DOTA. B) Relaxivity model sensor molecule, i.e. a cryptophane-A linked to **Gd**DOTA (**Rx** = CrA-**Gd**DOTA). C) DOTA protonation at pH = 0 causing dissociation of **Gd**^{III} from the molecule. (**Rx** = CrA-DOTA + **Gd**$^{III3+}$) D) **Rx** = **Gd**$^{III3+}$ in H_2O/ACN solution at pH = 7 and E) **Rx** = **Gd**^{III}-free precursor of the sensor molecule.

A 1 mM CrA-**Gd**DOTA solution corresponds to a $^{129}Xe_{(sol)}$ relaxation time of T_1 = 2.4 s that is sufficiently short to affect the overall relaxation *in vivo*. Unlike HyperCEST, this effect does not require radiofrequency irradiation for saturation to accomplish depolarization. Rather, depolarization occurs as the consequence of the combined effect of relaxation in the bound phase (i.e. ^{129}Xe in the cage) followed by chemical exchange leads to the fast decay of the dissolved phase signal. To deactivate the depolarization, the relaxation agent will need to be 'turned off' through selective chemical or biochemical cleavage of the paramagnetic center from the encapsulating cage.

To demonstrate the deactivation concept, but also to further prove that accelerated ^{129}Xe relaxation was indeed caused by the close vicinity of the paramagnetic metal to the encapsulated ^{129}Xe, HCl (37% v/v) was added to protonate DOTA and leach the **Gd**^{III} ion out of the chelator moiety to form CrA-DOTA + **Gd**$^{3+}_{(sol)}$. This process, led to a 4.3 fold drop in the relaxivity for ^{129}Xe to 0.0955 ±0.0051 $s^{-1}mM^{-1}$ shown in Fig. 3C. This value is still 2 times higher than that found for **Gd**DOTA in Fig. 3A, most likely because of increased contact of $^{129}Xe_{(sol)}$ with the unchelated paramagnetic metal ion (similarly effecting the ^{1}H relaxation in Fig. 3C). In a control experiment the relaxivity of $GdCl_3$ for ^{129}Xe in H_2O/ACN solution (Fig 3D, pH = 7) was found to be R_1/[**Rx**] = 0.0847 $s^{-1}mM^{-1}$, close to the value in Fig. 3C at pH = 0.

Fig. 2 also shows the time behavior (i – iii) of the DOTA protonation and the associated change in relaxivity that took several days for completion. This time behavior was verified through HPLC and mass spectrometry (see Supporting Information). It demonstrates that the change in relaxivity was indeed caused by the separation of the **Gd**^{III} center from the cryptophane cage and not by a pH dependence of the xenon in-out exchange rate with the cryptophane cage, in agreement with previous literature studying pH effects.[15]

Conclusions. The relaxation data generated in this study demonstrates a dramatic increase in relaxivity of a **Gd**DOTA for ^{129}Xe when the complex is tethered to a cryptophane cage. This increase is the consequence of the prolonged duration of cage bound ^{129}Xe in close vicinity to the paramagnetic metal center. The strong relaxation experienced by cage bound xenon is transferred through chemical exchange to the solvent phase ^{129}Xe. The dissolved phase ^{129}Xe signal decays at a rate that is the average of the relaxation rate in the cage and the relaxation rate in the solvent, scaled by the duration that the xenon atoms remain in the two respective phases.

As this hp ^{129}Xe chemical exchange relaxation transfer mechanism can be disrupted by the separation of CrA cage from the paramagnetic metal, a specifically designed responsive contrast agent can give rise to a new switchable ^{129}Xe depolarization based biosensor concept. Although this method may lack some of the intrinsic versatility of the HyperCEST concept, the presented responsive MRI contrast agent concept would not require high spectral resolution. In addition, switchable relaxation does not entail high power radiofrequency saturation that can be problematic for *in vivo* studies due to heat adsorption in tissue. Furthermore, the relaxation agent deactivation is ^{129}Xe specific and does not affect proton T_1 relaxation (compare Fig. 3, A and B) and standard ^{1}H T_1 relaxation maps should allow to probe for the presence of biosensors independent of the activation state. This should allow for differentiation of regions with higher concentration of deactivated biosensor from those with lower concentration of still active biosensor. Although both regions may result in similar ^{129}Xe relaxation rates, the very different ^{1}H relaxation behavior would enable correct interpretation.

The design of future responsive hp ^{129}Xe depolarization agents as potential biosensors deserves some consideration: In analogy to the r^{-6} dependence utilized in intramolecular Förster

resonance energy transfer (FRET),[16] the r^{-6} dependence of paramagnetic relaxation on distance r between the cage and the paramagnetic metal center could be exploited for sensors that operate through conformational changes or through a cleavable linker between the two groups. Enzymatic cleavage of the linker between paramagnetic **Gd**DOTA and a ^{19}F containing reporter group was previously utilized to deactivate paramagnetic T_2 relaxation, thereby reducing line broadening in thermally polarized ^{19}F NMR.[17] Furthermore, enzymatic cleavage has been detected through a chemical shift based hp ^{129}Xe biosensor.[18] Similarly, cleavable linkers between a paramagnetic group and cryptophane cage may provide a usable responsive hp ^{129}Xe relaxation agents. The molecular design of the hp ^{129}Xe depolarization based biosensors can be advanced through an increase in the number of captured xenon atoms, for example through the usage of multiple cryptophane cages or through capsides[19] that would also increase rotational correlation times. Both effects will likely increase the relaxivity of the activated state but not of the deactivated state. Finally, $\mathbf{Gd}^{III}$ can be substituted by other paramagnetic groups with stronger relaxation properties such as Mn(II) nanoparticles.[20]

Experimental Section

As described in detail in the Supporting Information, the model sensor CrA-**Gd**DOTA was synthesized from a DOTA chelator, modified with a short linker, and cryptophanol. Cryptophanol was synthesized as previously reported by Bertault and co-workers,[7d] while the DOTA-linker was simply obtained by reacting an appropriately protected DO3A with a short bisamide linker with *alpha*-bromoacetyl as terminal. The cryptophanol was then reacted with the *alpha*-bromoacetyl group to form an ether. After deprotection of the DOTA carboxylic groups, the $\mathbf{Gd}^{III}$ cation was successfully chelated, yielding the desired compound CrA-**Gd**DOTA.

All NMR relaxation measurements were obtained at a temperature of 293 K at 9.4 T field strength. Hp ^{129}Xe was produced through spin exchange optical pumping (SEOP) using a custom–built instrument described elsewhere.[21] Prior to hp ^{129}Xe delivery in each experiment the solution was purged with N_2 for 2 min to ensure the removal of any residual O_2. The hp gas mixture was then delivered under continuous flow SEOP conditions for 45 s at 40 ml/min into the relaxation agent containing solution. After flow stoppage, the dissolved phase hp ^{129}Xe T_1 relaxation was measured through a sequence of 16 constant flip angle (12°) experiments.[22] A standard inversion recovery sequence was used to obtain the ^1H T_1 relaxation of H_2O.

Acknowledgements

This work was supported in parts by the Medical Research Council under Grant No. G0900785, by the Royal Society through the Paul Instrument Fund, through the EPSRC Research Development Fund – Bridging the Gaps, and the BBSRC Sparking Impact Award.

Keywords: Hyperpolarized xenon biosensor • MRI contrast agent • cryptophane • HyperCEST • molecular imaging

[1] E. Terreno, D. Delli Castelli, A. Viale, S. Aime, *Chem Rev* **2010**, *110*, 3019-3042.

[2] a.) M. M. Spence, S. M. Rubin, I. E. Dimitrov, E. J. Ruiz, D. E. Wemmer, A. Pines, S. Q. Yao, F. Tian, P. G. Schultz, *P Natl Acad Sci USA* **2001**, *98*, 10654-10657; b.) M. M. Spence, E. J. Ruiz, S. M. Rubin, T. J. Lowery, N. Winssinger, P. G. Schultz, D. E. Wemmer, A. Pines, *J Am Chem Soc* **2004**, *126*, 15287-15294; c.) L. Schroder, T. J. Lowery, C. Hilty, D. E. Wemmer, A. Pines, *Science* **2006**, *314*, 446-449.

[3] a.) P. Berthault, G. Huber, H. Desvaux, *Progress in Nuclear Magnetic Resonance Spectroscopy* **2009**, *55*, 35-60; b.) O. Taratula, I. J. Dmochowski, *Current Opinion in Chemical Biology* **2010**, *14*, 97-104; c.) D. M. L. Lilburn, G. E. Pavlovskaya, T. Meersmann, *J Magn Reson* **2012**.

[4] Y. B. Bai, Y. F. Wang, M. Goulian, A. Driks, I. J. Dmochowski, *Chem Sci* **2014**, *5*, 3197-3203.

[5] C. Witte, V. Martos, H. M. Rose, S. Reinke, S. Klippel, L. Schroder, C. P. R. Hackenberger, *Angew Chem Int Edit* **2015**, *54*, 2806-2810.

[6] J. M. Chambers, P. A. Hill, J. A. Aaron, Z. H. Han, D. W. Christianson, N. N. Kuzma, I. J. Dmochowski, *J Am Chem Soc* **2009**, *131*, 563-569.

[7] a.) V. Roy, T. Brotin, J. P. Dutasta, M. H. Charles, T. Delair, F. Mallet, G. Huber, H. Desvaux, Y. Boulard, P. Berthault, *Chemphyschem* **2007**, *8*, 2082-2085; b.) G. K. Seward, Q. Wei, I. J. Dmochowski, *Bioconjugate Chemistry* **2008**, *19*, 2129-2135; c.) A. Schlundt, W. Kilian, M. Beyermann, J. Sticht, S. Gunther, S. Hopner, K. Falk, O. Roetzschke, L. Mitschang, C. Freund, *Angew Chem Int Edit* **2009**, *48*, 4142-4145; d.) C. Boutin, A. Stopin, F. Lenda, T. Brotin, J. P. Dutasta, N. Jamin, A. Sanson, Y. Boulard, F. Leteurtre, G. Huber, A. Bogaert-Buchmann, N. Tassali, H. Desvaux, M. Carriere, P. Berthault, *Bioorgan Med Chem* **2011**, *19*, 4135-4143; e.) K. K. Palaniappan, R. M. Ramirez, V. S. Bajaj, D. E. Wemmer, A. Pines, M. B. Francis, *Angew Chem Int Edit* **2013**, *52*, 4849-4853.

[8] H. M. Rose, C. Witte, F. Rossellaa, S. Klippel, C. Freund, L. Schroder, *P Natl Acad Sci USA* **2014**, *111*, 11697-11702.

[9] F. Lerouge, O. Melnyk, J. O. Durand, L. Raehm, P. Berthault, G. Huber, H. Desvaux, A. Constantinesco, P. Choquet, J. Detour, M. Smaihi, *Journal of Materials Chemistry* **2009**, *19*, 379-386.

[10] a.) E. Terreno, M. Botta, P. Boniforte, C. Bracco, L. Milone, B. Mondino, F. Uggeri, S. Aime, *Chem-Eur J* **2005**, *11*, 5531-5537; b.) R. B. van Heeswijk, S. Laus, F. D. Morgenthaler, R. Gruetter, *Magnetic Resonance Imaging* **2007**, *25*, 821-825; c.) C. Gabellieri, M. O. Leach, T. R. Eykyn, *Contrast Media Mol I* **2009**, *4*, 143-147; d.) R. B. van Heeswijk, K. Uffmann, A. Comment, F. Kurdzesau, C. Perazzolo, C. Cudalbu, S. Jannin, J. A. Konter, P. Hautle, B. van den Brandt, G. Navon, J. J. van der Klink, R. Gruetter, *Magn Reson Med* **2009**, *61*, 1489-1493; e.) R. T. Branca, Z. I. Cleveland, B. Fubara, C. S. S. R. Kumar, R. R. Maronpot, C. Leuschner, W. S. Warren, B. Driehuys, *P Natl Acad Sci USA* **2010**, *107*, 3693-3697.

[11] M. Gomes, P. Dao, C. Slack, C. Vassiliou, A. Truxal, K. Jeong, D. E. Wemmer, M. B. Francis, A. Pines, in *56th Experimental NMR Conference, April 19 - 24*, Asilomar, **2015**.

[12] a.) A. Abragam, *The Principles of Nuclear Magnetism*, Oxford University Press, Oxford, UK, **1961**; b.) N. Bloembergen, L. O. Morgan, *J Chem Phys* **1961**, *34*, 842-&.

[13] J. P. Mugler, T. A. Altes, *J Magn Reson Imaging* **2013**, *37*, 313-331.

[14] a.) M. S. Albert, D. F. Kacher, D. Balamore, A. K. Venkatesh, F. A. Jolesz, *J Magn Reson* **1999**, *140*, 264-273; b.) J. Wolber, A. Cherubini, A. S. K. Dzik-Jurasz, M. O. Leach, A. Bifone, *P Natl Acad Sci USA* **1999**, *96*, 3664-3669; c.) G. Norquay, G. Leung, N. J. Stewart, G. M. Tozer, J. Wolber, J. M. Wild, *Magn Reson Med* **2014**, *DOI: 10.1002/mrm.25417*.

[15] P. Berthault, H. Desvaux, T. Wendlinger, M. Gyejacquot, A. Stopin, T. Brotin, J. P. Dutasta, Y. Boulard, *Chem-Eur J* **2010**, *16*, 12941-12946.

[16] J. Zhang, R. E. Campbell, A. Y. Ting, R. Y. Tsien, *Nat Rev Mol Cell Bio* **2002**, *3*, 906-918.

[17] a.) A. Y. Louie, M. M. Huber, E. T. Ahrens, U. Rothbacher, R. Moats, R. E. Jacobs, S. E. Fraser, T. J. Meade, *Nat Biotech* **2000**, *18*, 321-325; b.) S. Mizukami, R. Takikawa, F. Sugihara, Y. Hori, H. Tochio, M. Walchli, M. Shirakawa, K. Kikuchi, *Journal of the American Chemical Society* **2008**, *130*, 794-+; c.) U. Himmelreich, S. Aime, T. Hieronymus, C. Justicia, F. Uggeri, M. Zenke, M. Hoehn, *Neuroimage* **2006**, *32*, 1142-1149; d.) W. Cui, P. Otten, Y. Li, K. S. Koeneman, J. Yu, R. P. Mason, *Magn Reson Med* **2004**,

51, 616-620; e.) Y. Takaoka, T. Sakamoto, S. Tsukiji, M. Narazaki, T. Matsuda, H. Tochio, M. Shirakawa, I. Hamachi, *Nat Chem* **2009**, *1*, 557-561; f.) X. Y. Yue, Z. Wang, L. Zhu, Y. Wang, C. Q. Qian, Y. Ma, D. O. Kiesewetter, G. Niu, X. Y. Chen, *Mol Pharmaceut* **2014**, *11*, 4208-4217.

[18] Q. Wei, G. K. Seward, P. A. Hill, B. Patton, I. E. Dimitrov, N. N. Kuzma, I. J. Dmochowski, *J Am Chem Soc* **2006**, *128*, 13274-13283.

[19] a.) T. Meldrum, K. L. Seim, V. S. Bajaj, K. K. Palaniappan, W. Wu, M. B. Francis, D. E. Wemmer, A. Pines, *Journal of the American Chemical Society* **2010**, *132*, 5936-5937; b.) T. Stevens, K. Palaniappan, R. Ramirez, M. Francis, D. Wemmer, A. Pines, *Magnetic Resonance in Medicine* **2013**, *69*, 1245–1252

[20] J. M. Shin, R. M. Anisur, M. K. Ko, G. H. Im, J. H. Lee, I. S. Lee, *Angew Chem Int Edit* **2009**, *48*, 321-324.

[21] a.) J. S. Six, T. Hughes-Riley, K. F. Stupic, G. E. Pavlovskaya, T. Meersmann, *Plos One* **2012**, *7*; b.) K. F. Stupic, J. S. Six, M. D. Olsen, G. E. Pavlovskaya, T. Meersmann, *Phys Chem Chem Phys* **2013**, *15*, 94-97; c.) T. Hughes-Riley, J. S. Six, D. M. L. Lilburn, K. F. Stupic, A. C. Dorkes, D. E. Shaw, G. E. Pavlovskaya, T. Meersmann, *J Magn Reson* **2013**, *237*, 23-33.

[22] K. F. Stupic, N. D. Elkins, G. E. Pavlovskaya, J. E. Repine, T. Meersmann, *Physics in Medicine and Biology* **2011**, *56*, 3731-3748.

WILEY-VCH

Entry for the Table of Contents (Please choose one layout)

Layout 1:

COMMUNICATION

The relaxivity of paramagnetic **Gd**DOTA for ^{129}Xe was dramatically increased through tethering to a cryptophane cage, providing the path for a responsive depolarization agent.

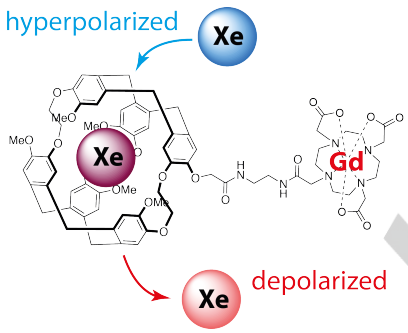

*Author(s), Corresponding Author(s)**

Page No. – Page No.

Title

Layout 2:

COMMUNICATION

((Insert TOC Graphic here))

*Author(s), Corresponding Author(s)**

Page No. – Page No.

Title

Text for Table of Contents

WILEY-VCH